

Numerical Heat Transfer, Part B: Fundamentals



ISSN: 1040-7790 (Print) 1521-0626 (Online) Journal homepage: http://www.tandfonline.com/loi/unhb20

NEW FAMILY OF ADAPTIVE VERY HIGH RESOLUTION SCHEMES

F. Moukalled & M. S. Darwish

To cite this article: F. Moukalled & M. S. Darwish (1998) NEW FAMILY OF ADAPTIVE VERY HIGH RESOLUTION SCHEMES, Numerical Heat Transfer, Part B: Fundamentals, 34:2, 215-239

To link to this article: http://dx.doi.org/10.1080/10407799808915055



Full Terms & Conditions of access and use can be found at http://www.tandfonline.com/action/journalInformation?journalCode=unhb20

NEW FAMILY OF ADAPTIVE VERY HIGH RESOLUTION SCHEMES

F. Moukalled and M. S. Darwish

Faculty of Engineering and Architecture, Mechanical Engineering Department, American University of Beirut, P.O. Box 11-0236, Beirut, Lebanon

The family of skew very high resolution (VHR) schemes is adaptively combined with the family of high-resolution (HR) schemes to yield a new family of adaptive very high resolution (AVHR) schemes. A new simple adaptive switching criterion is devised. For convection-diffusion type problems the adaptive schemes are accelerated by using in tandem the normalized weighting factor method to implement the HR scheme and the deferred-correction (DC) procedure to implement the skew scheme. For flow problems the DC procedure is used to implement both types of schemes. Numerical results for the new family of AVHR schemes are compared in terms of accuracy and computation cost against those generated using the VHR base family of schemes by solving four problems: (1) pure convection of a step profile in an oblique velocity field, (2) driven flow in a skew cavity, (3) laminar sudden expansion of an oblique velocity field in a rectangular cavity. For the same accuracy, the AVHR schemes are found to decrease the computation cost, on average, by 48.74% as compared to the VHR schemes.

INTRODUCTION

An extensive amount of research in computational fluid dynamics has been directed toward the development of accurate and bounded convective schemes. The outcome of the various studies has allowed a deep understanding and effective remedies of the problems involved and has resulted in a large number of one-dimensional high resolution (HR) [1–9] and multidimensional very high resolution (VHR) [10, 11] schemes. Published work [11] has shown that HR schemes largely decrease errors produced by streamwise numerical diffusion and, to a lesser extent, errors arising from cross-stream numerical diffusion, whereas VHR schemes greatly reduce both components of numerical diffusion. Moreover, enforcing a monotonicity criterion has minimized errors arising from numerical dispersion. The total variation diminishing (TVD) scheme is one framework for developing HR schemes [4, 12]. Another more recent and elegant framework is the normalized variable formulation (NVF) methodology of Leonard [8] and its extension, the normalized variable and space formulation (NVSF) methodology of Darwish and Moukalled [13].

Received 18 December 1997; accepted 17 March 1998.

Address correspondence to F. Moukalled, Faculty of Engineering and Architecture, Mechanical Engineering Department, American University of Beirut, P.O. Box 11-0236, Beirut, Lebanon. E-mail: memouk@aub.edu.lb

	NOMENO	CLATU	RE
a	coefficients of the discretized	ξ, η	curvilinear coordinates
	equation .	ρ	density
3	volume integral of the Q source term convective flux coefficient	φ	general dependent variable
γ() g ^ε , g ^η	functional relationship local contravariant unit vectors	Subscripts	
;	geometric factor	С	central grid point
GRAD	gradient across a control volume face	D	downstream grid point
GRAD	normalized gradient across a control	dc	deferred correction
	volume face	f	refers to control volume face
	total scalar flux across cell face	nb	refers to neighbors
) RE	source term residual error	U	upstream grid point
LOPE	surface area of the control volume parameter representing the skewness	Superscripts	
	of the flow with respect to the grid	С	convection contribution
,	volume of the control volume	D	diffusion contribution
7	velocity vector	φ	refers to dependent variable
Γ	diffusion coefficient	~	refers to normalized variable

The work of Moukalled and Darwish [10, 11] that has led to the development of the family of VHR schemes can be viewed as an extension of the family of one-dimensional HR schemes developed in the context of the NVSF methodology into multidimensional spaces. This family was shown [10, 11] to be by far more accurate than the HR family in situations when the flow is oblique to the grid lines along with important gradients in the flow. Moreover, the two families were found to be of equal accuracy in situations when the flow is more or less aligned with the grid network. The VHR multidimensional schemes are definitely more expensive to compute than the one-dimensional HR schemes, since they require additional interpolation steps to determine the upstream, central, and downstream values in the flow direction and because of the expanded stencil of nodes used in the interpolation. Since the accuracy of both schemes is the same in regions where the flow is more or less aligned with the grid lines, it is not necessary to use them there. Therefore the same overall accuracy could be achieved at a lower cost through an adaptive strategy.

To this end, a new family of adaptive schemes is developed in this work. The adaptive method switches to the skew VHR scheme in the presence of a high change in the gradient of the dependent variable in combination with the flow being oblique to the grid line and to the one-dimensional HR scheme elsewhere. Thus the expensive VHR schemes are used only where needed, while the cheaper HR schemes are used in the remaining computational regions. Few attempts based on the TVD approach to develop composite adaptive schemes have been reported [14]. Rhodes and Acharya [15] developed a solution-adaptive differencing scheme within a multigrid-type calculation procedure. In their work the upwind scheme was used over the outer grid and the third-order Quick scheme in the flagged

regions. Some work has also been done in the context of the NVF methodology [16]. However, to the authors' knowledge, no work related to developing adaptive one-dimensional/multidimensional schemes has been reported in the literature. Moreover, a new criterion is devised for selecting the type of scheme to be used along a control volume face. The adaptive strategy is applied to the following schemes in their one-dimensional and multidimensional [11] forms: CLAM [1], MUSCL [2], OSHER [3], MINMOD [4], SHARP [5], SMART [6], STOIC [7], EXPONENTIAL [8], and SUPERC [9].

In what follows, the discretization procedure will first be presented along with a brief description of the NVSF methodology. Then the construction of the HR and VHR schemes is detailed, the adaptive strategy and criterion explained, and the resultant adaptive very high resolution (AVHR) schemes tested and compared in terms of speed and accuracy with their VHR counterparts by solving four problems: (1) pure convection of a step profile in an oblique velocity field, (2) driven flow in a skew cavity, (3) laminar sudden expansion of an oblique velocity field in a rectangular cavity, and (4) turbulent sudden expansion of an oblique velocity field in a rectangular cavity. In solving the convective problem, the AVHR schemes are accelerated by using in tandem the recently developed normalized weighting factor (NWF) technique [17] to implement the HR schemes and the deferred-correction (DC) method [18] to implement the skew schemes. For flow problems, however, the AVHR schemes are implemented using the DC method only.

CONTROL VOLUME DISCRETIZATION OF THE TRANSPORT EQUATIONS

The conservation equations governing two-dimensional incompressible steady flow problems may be expressed in the following general form:

$$\nabla \cdot (\rho \nabla \phi - \Gamma^{\phi} \nabla \phi) = O^{\phi} \tag{1}$$

where ϕ is any dependent variable, V is the velocity vector, ρ is density, and Γ^{ϕ} and Q^{ϕ} , specific to a particular meaning of ϕ , are the diffusivity and source term, respectively. Since a control-volume-based numerical approach is used, the integral form of Eq. (1) is sought. For this purpose, Eq. (1) is first integrated over the control volume shown in Figure 1a, and then the divergence theorem is applied on the resultant equation to yield

$$\oint_{S} (\rho V \phi - \Gamma^{\phi} \nabla \phi) dS = \int_{V} Q dV$$
 (2)

where S and V are the surface area and the volume of the control volume (Figure 1a). Replacing the surface integral over the control volume by a discrete

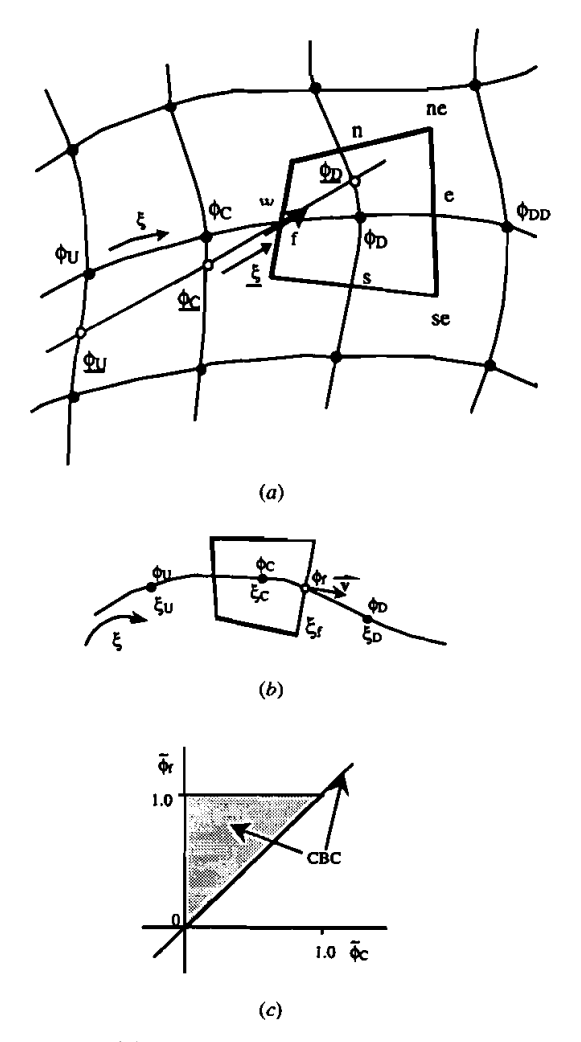


Figure 1. (a) Typical grid point cluster, control volume, and skew interpolation. (b) Interpolation points used in calculating ϕ_f . (c) Convective boundedness criterion (CBC) on the normalized variable diagram.

summation of the flux terms over the sides of the control volume, Eq. (2) becomes

$$J_{\rm e} - J_{\rm w} + J_{\rm n} - J_{\rm s} = B \tag{3}$$

where B is the volume integral of the source term Q^{ϕ} and $J_{\rm f}$ represents the total flux of ϕ across cell face "f" (f = e, w, n, or s) and is given by

$$J_{\rm f} = (\rho V \phi - \Gamma^{\phi} \nabla \phi)_{\rm f} S_{\rm f} \tag{4}$$

Each of the surface fluxes $J_{\rm f}$ contains a convective contribution $J_{\rm f}^{\rm C}$ and a diffusive contribution $J_{\rm f}^{\rm D}$; hence

$$J_f = J_f^{\mathcal{C}} + J_f^{\mathcal{D}} \qquad J_f^{\mathcal{C}} = (\rho V \phi)_f S_f \qquad J_f^{\mathcal{D}} = (-\Gamma^{\phi} \nabla \phi)_f S_f \tag{5}$$

The accuracy of the control volume solution depends on the proper estimation of the face value of ϕ as a function of the neighboring ϕ node values. Through the use of an interpolation profile, the approximation scheme produces an expression for the face value that is dependent on the nodal ϕ values in the vicinity of the face.

The diffusion flux $J_{\rm f}^{\rm D}$ is discretized along each surface of the control volume. The procedure is explained here by discretizing the gradient $\nabla \phi$ along the east face (face e) of the control volume shown in Figure 1a. For a Cartesian coordinate system the gradient $\nabla \phi$ for the east control volume face is given by

$$(\nabla \phi)_{c} = \left(\frac{\partial \phi}{\partial x}\right)_{c} i + \left(\frac{\partial \phi}{\partial y}\right)_{c} j \tag{6}$$

Since the new AVHR schemes are also tested in nonconventional geometry, a general curvilinear boundary-fitted coordinate system is used. In such a coordinate system, the control volumes are arbitrary in shape, and the gradient needs to be determined along local curvilinear coordinates. Using the curvilinear coordinates (ξ, η) and the local contravariant unit vectors (g^{ξ}, g^{η}) (normal to the coordinate surfaces), $(\nabla \phi)_c$ is transformed to

$$(\nabla \phi)_{e} = \left(\frac{\partial \phi}{\partial \xi}\right)_{e} \mathbf{g}_{e}^{\xi} + \left(\frac{\partial \phi}{\partial \eta}\right)_{e} \mathbf{g}_{e}^{\eta} \tag{7}$$

Without loss of generality, the increments in (ξ, η) space may arbitrarily be chosen as 1. Thus the discretized expressions for the normal and cross derivatives are

$$\frac{\partial \phi}{\partial \xi}\bigg|_{e} = \frac{\phi_{DD} - \phi_{D}}{1} = \phi_{DD} - \phi_{D} \qquad \frac{\partial \phi}{\partial \eta}\bigg|_{e} = \frac{(\phi_{n} - \phi_{s})_{e}}{1} = \phi_{ne} - \phi_{se} \quad (8)$$

respectively. Combining Eqs. (7) and (8), the equation for $(\nabla \phi)_e$ becomes

$$(\nabla \phi)_e = (\phi_{\rm DD} - \phi_{\rm D}) \mathbf{g}_e^{\xi} + (\phi_{\rm ne} - \phi_{\rm se}) \mathbf{g}_e^{\eta} \tag{9}$$

Using Eq. (9), the discretized form of the diffusion flux is found to be

$$J_{\rm e}^{\rm D} = -\Gamma_{\rm e}^{\phi} \left[G_{\rm e}^{\rm ND} (\phi_{\rm DD} - \phi_{\rm D})_{\rm e} + G_{\rm e}^{\rm CD} (\phi_{\rm ne} - \phi_{\rm se}) \right]$$
 (10)

where G_e^{ND} and G_e^{CD} are the geometric factors for normal and cross diffusion, respectively.

The convective flux across face f can be written as

$$J_f^{C} = (\rho \mathbf{V}\phi)_f S_f = C_f \phi_f \tag{11}$$

where $C_{\rm f}$ is the convective flux coefficient. As can be seen from Eq. (11), the accuracy of the control volume solution for the convective scalar flux depends on the proper estimation of the face value $\phi_{\rm f}$ as a function of the neighboring ϕ nodes values. The estimation of $\phi_{\rm f}$ is the main concern of this work. Using some assumed interpolation profile, $\phi_{\rm f}$ can be explicitly formulated in terms of the nodal values by a functional relationship of the form

$$\phi_{\rm f} = f(\phi_{\rm nb}) \tag{12}$$

where ϕ_{nb} denotes the ϕ values at the neighboring nodes. The interpolation profile may be one-dimensional or multidimensional of low or high order of accuracy. The higher the order of the profile, the lower the numerical diffusion will be. However, the order of the profile and its dimensionality do not eliminate numerical dispersion.

After substituting Eq. (12) into Eq. (11) for each cell face and using the resulting equation along with Eq. (10), Eq. (3) is transformed after some algebraic manipulations into the following discretized equation:

$$a_{\rm D}\phi_{\rm D} = \sum_{\rm nb} (a_{\rm nb}\phi_{\rm nb}) + b_{\rm D}$$
 (13)

where the coefficients a_D and a_{nb} depend on the selected scheme and b_D is the source term of the discretized equation. An equation similar to Eq. (13) is obtained at each grid point in the domain, and the collection of all these equations forms a system of algebraic equations that is solved here iteratively to obtain the ϕ field.

So far, the velocity field has been assumed to be known, and the methodology to solve for a scalar variable has been presented. For some of the problems considered here, the flow field is unknown. Therefore, to obtain the solution, the continuity and momentum equations should be solved simultaneously. These equations are solved in this work on a nonstaggered grid, and unrealistic checkerboard pressure and velocity fields are avoided through the use of the pressure-weighted interpolation method of Peric [19]. Moreover, since the pressure is implicitly specified by the continuity constraint, a pressure-correction equation is derived by combining the momentum and continuity equations as in the SIMPLEC algorithm [20], which is a variation of the SIMPLE algorithm of Patankar [21].

NORMALIZED VARIABLES AND CONVECTION BOUNDEDNESS CRITERION

As mentioned above, increasing the order and/or dimensionality of the interpolation profile does not eliminate errors caused by numerical dispersion. To

minimize this error, limiters on the convective flux should be imposed. The flux limiter denoted by the convective boundedness criterion (CBC) [6] is adopted here and explained next in terms of the normalized variables approach. Figure 1b shows the local behavior of the convected variable near a control volume face. If the value of the dependent variable at the control volume face located at a distance ξ_f from the origin is expressed by ϕ_f , then the normalized variables will be defined as [13]

$$\tilde{\phi} = \frac{\phi - \phi_{\mathrm{U}}}{\phi_{\mathrm{D}} - \phi_{\mathrm{U}}} \qquad \tilde{\xi} = \frac{\xi - \xi_{\mathrm{U}}}{\xi_{\mathrm{D}} - \xi_{\mathrm{U}}} \tag{14}$$

where the subscripts U and D, which depend on the flow direction, refer to upstream and downstream nodal locations, respectively. Using the normalized variables, the convection boundedness criterion for implicit steady state flow calculation [6] states that for a scheme to have the boundedness property its functional relationship should be continuous and bounded from below by $\tilde{\phi}_f = \tilde{\phi}_C$ and from above by unity, should pass through the point (0,0) and (1,1) in the monotonic range $0 < \tilde{\phi}_C < 1$, and for $\tilde{\phi}_C < 0$ or $\tilde{\phi}_C > 1$ the functional relationship $f(\tilde{\phi}_C)$ should equal $\tilde{\phi}_C$. The above conditions may also be described geometrically on a normalized variable diagram (NVD) as shown in Figure 1c. Since the intention of the present work is to develop adaptive schemes based on one-dimensional HR and multidimensional VHR schemes, these are reviewed next.

HIGH-RESOLUTION SCHEMES

Knowing the required conditions for boundedness, the shortcomings of the unbounded high-order schemes were eliminated through the development of HR schemes satisfying all the above requirements. Without going into details, a number of HR schemes were formulated using the NVSF methodology, and the functional relationships for those used in this work are given below. For more details, the reader is referred to Darwish and Moukalled [13].

MINMOD

$$\tilde{\phi} = \frac{\tilde{\xi}_{f}}{\tilde{\xi}_{C}} \tilde{\phi}_{C} \qquad 0 < \tilde{\phi}_{C} < \tilde{\xi}_{C}$$

$$\tilde{\phi}_{f} = \frac{1 - \tilde{\xi}_{f}}{1 - \tilde{\xi}_{C}} \tilde{\phi}_{C} + \frac{\tilde{\xi}_{f} - \tilde{\xi}_{C}}{1 - \tilde{\xi}_{C}} \qquad \tilde{\xi}_{C} < \tilde{\phi}_{C} < 1$$

$$\tilde{\phi}_{f} = \tilde{\phi}_{C} \qquad \text{elsewhere}$$

$$(15)$$

OSHER

$$\tilde{\phi}_{f} = \frac{\tilde{\xi}_{f}}{\tilde{\xi}_{C}} \tilde{\phi}_{C} \qquad 0 < \tilde{\phi}_{C} < \frac{\tilde{\xi}_{C}}{\tilde{\xi}_{f}}$$

$$\tilde{\phi}_{f} = 1 \qquad \frac{\tilde{\xi}_{C}}{\tilde{\xi}_{f}} \leqslant \tilde{\phi}_{C} < 1$$

$$\tilde{\phi}_{f} = \tilde{\phi}_{C} \qquad \text{elsewhere}$$
(16)

EXPONENTIAL

$$\tilde{\phi}_{\rm f} = 1.125(1 - e^{-2.19722\tilde{\phi}_{\rm C}}) \qquad 0 < \tilde{\phi}_{\rm C} < 1$$

$$\tilde{\phi}_{\rm f} = \tilde{\phi}_{\rm C} \qquad \qquad \text{elsewhere}$$

$$(17)$$

MUSCL

$$\tilde{\phi}_{f} = \frac{2\,\tilde{\xi}_{f} - \tilde{\xi}_{C}}{\tilde{\xi}_{C}}\,\tilde{\phi}_{C} \qquad 0 < \tilde{\phi}_{C} < \frac{\tilde{\xi}_{C}}{2}$$

$$\tilde{\phi}_{f} = \tilde{\phi}_{C} + \left(\tilde{\xi}_{f} - \tilde{\xi}_{C}\right) \qquad \frac{\tilde{\xi}_{C}}{2} \leq \tilde{\phi}_{C} < 1 + \tilde{\xi}_{C} - \tilde{\xi}_{f} \qquad (18)$$

$$\tilde{\phi}_{f} = 1 \qquad 1 + \tilde{\xi}_{C} - \tilde{\xi}_{f} \leq \tilde{\phi}_{C} < 1$$

$$\tilde{\phi}_{f} = \tilde{\phi}_{C} \qquad \text{elsewhere}$$

CLAM

$$\tilde{\phi}_{f} = \frac{\left(\tilde{\xi}_{C}^{2} - \tilde{\xi}_{f}\right)}{\tilde{\xi}_{C}\left(\tilde{\xi}_{C} - 1\right)}\tilde{\xi}_{C} + \frac{\left(\tilde{\xi}_{f} - \tilde{\xi}_{C}\right)}{\tilde{\xi}_{C}\left(\tilde{\xi}_{C} - 1\right)}\tilde{\xi}_{C}^{2} \qquad 0 < \tilde{\phi}_{C} < 1$$

$$\tilde{\phi}_{f} = \tilde{\phi}_{C} \qquad \text{elsewhere}$$

SMART

$$\tilde{\phi}_{f} = \frac{\tilde{\xi}_{f} \left(1 - 3\tilde{\xi}_{C} + 2\tilde{\xi}_{f}\right)}{\tilde{\xi}_{C} \left(1 - \tilde{\xi}_{C}\right)} \tilde{\phi}_{C} \qquad 0 < \tilde{\phi}_{C} < \frac{\tilde{\xi}_{C}}{3}$$

$$\tilde{\phi}_{f} = \frac{\tilde{\xi}_{f} \left(1 - \tilde{\xi}_{f}\right)}{\tilde{\xi}_{C} \left(1 - \tilde{\xi}_{C}\right)} \tilde{\phi}_{C} + \frac{\tilde{\xi}_{f} \left(\tilde{\xi}_{f} - \tilde{\xi}_{C}\right)}{1 - \tilde{\xi}_{C}} \qquad \frac{\tilde{\xi}_{C}}{3} \le \tilde{\phi}_{C} < \frac{\tilde{\xi}_{C}}{\tilde{\xi}_{f}} \left(1 + \tilde{\xi}_{f} - \tilde{\xi}_{C}\right)$$

$$\tilde{\phi}_{f} = 1 \qquad \qquad \frac{\tilde{\xi}_{C}}{\tilde{\xi}_{f}} \left(1 + \tilde{\xi}_{f} - \tilde{\xi}_{C}\right) \le \tilde{\phi}_{C} < 1$$

$$\tilde{\phi}_{f} = \tilde{\phi}_{C} \qquad \text{elsewhere}$$

SHARP

$$\tilde{\phi}_{f} = \frac{\tilde{\xi}_{f}(\tilde{\xi}_{f} - \tilde{\xi}_{C})}{1 - \tilde{\xi}_{C}} + \frac{\tilde{\xi}_{f}(\tilde{\xi}_{f} - 1)}{\tilde{\xi}_{C}(\tilde{\xi}_{C} - 1)}\tilde{\phi}_{C} \qquad \tilde{\phi}_{C} = 0.5$$

$$\tilde{\phi}_{f} = \frac{\sqrt{\tilde{\phi}_{C}(1 - \tilde{\phi}_{C})^{3}} - \tilde{\phi}_{C}^{2}}{1 - 2\tilde{\phi}_{C}} \qquad 0 \leqslant \tilde{\phi}_{C} < 1 \qquad \tilde{\phi}_{C} \neq 0.5$$

$$\tilde{\phi}_{f} = \tilde{\phi}_{C} \qquad \text{elsewhere}$$

STOIC

$$\tilde{\phi}_{f} = \frac{\tilde{\xi}_{f} \left(1 - 3\tilde{\xi}_{C} + 2\tilde{\xi}_{f}\right)}{\tilde{\xi}_{C} \left(1 - \tilde{\xi}_{C}\right)} \tilde{\phi}_{C} \qquad 0 < \tilde{\phi}_{C} < \frac{\tilde{\xi}_{C} \left(\tilde{\xi}_{C} - \tilde{\xi}_{f}\right)}{\tilde{\xi}_{C} + 2\tilde{\xi}_{f}^{2} - 4\tilde{\xi}_{f}^{2}\tilde{\xi}_{C}}$$

$$\tilde{\phi}_{f} = \frac{1 - \tilde{\xi}_{f}}{1 - \tilde{\xi}_{C}} \tilde{\phi}_{C} + \frac{\tilde{\xi}_{f} - \tilde{\xi}_{C}}{1 - \tilde{\xi}_{C}} \qquad \frac{\tilde{\xi}_{C} \left(\tilde{\xi}_{C} - \tilde{\xi}_{f}\right)}{\tilde{\xi}_{C} + \tilde{\xi}_{f}^{2} + 2\tilde{\xi}_{f}^{2} - 4\tilde{\xi}_{f}^{2}\tilde{\xi}_{C}} \leq \tilde{\phi}_{C} < \tilde{\xi}_{C}$$

$$\tilde{\phi}_{f} = \frac{\tilde{\xi}_{f} \left(1 - \tilde{\xi}_{f}\right)}{\tilde{\xi}_{C} \left(1 - \tilde{\xi}_{C}\right)} \tilde{\phi}_{C} + \frac{\tilde{\xi}_{f} \left(\tilde{\xi}_{f} - \tilde{\xi}_{C}\right)}{1 - \tilde{\xi}_{C}} \qquad \tilde{\xi}_{C} \leq \tilde{\phi}_{C} < \frac{\tilde{\xi}_{C}}{\tilde{\xi}_{f}} \left(1 + \tilde{\xi}_{f} - \tilde{\xi}_{C}\right)$$

$$\tilde{\phi}_{f} = 1 \qquad \qquad \frac{\tilde{\xi}_{C}}{\tilde{\xi}_{f}} \left(1 + \tilde{\xi}_{f} - \tilde{\xi}_{C}\right) < \tilde{\phi}_{C} < 1$$

$$\tilde{\phi}_{f} = \tilde{\phi}_{C} \qquad \text{elsewhere}$$

SUPERC

$$\tilde{\phi}_{f} = \frac{\tilde{\xi}_{f} \left(1 - 3\tilde{\xi}_{C} + 2\tilde{\xi}_{f}\right)}{\tilde{\xi}_{C} \left(1 - \tilde{\xi}_{C}\right)} \tilde{\phi}_{C} \qquad 0 < \tilde{\phi}_{C} < \frac{2}{5} \tilde{\xi}_{C}$$

$$\tilde{\phi}_{f} = \frac{1 - \tilde{\xi}_{f}}{1 - \tilde{\xi}_{C}} \tilde{\phi}_{C} + \frac{\tilde{\xi}_{f} - \tilde{\xi}_{C}}{1 - \tilde{\xi}_{C}} \qquad \frac{2}{5} \tilde{\xi}_{C} \leq \tilde{\phi}_{C} < \tilde{\xi}_{C}$$

$$\tilde{\phi}_{f} = \frac{\tilde{\xi}_{f} \left(1 - \tilde{\xi}_{f}\right)}{\tilde{\xi}_{C} \left(1 - \tilde{\xi}_{C}\right)} \tilde{\phi}_{C} + \frac{\tilde{\xi}_{f} \left(\tilde{\xi}_{f} - \tilde{\xi}_{C}\right)}{1 - \tilde{\xi}_{C}} \qquad \tilde{\xi}_{C} \leq \tilde{\phi}_{C} < \frac{\tilde{\xi}_{C}}{\tilde{\xi}_{f}} \left(1 + \tilde{\xi}_{f} - \tilde{\xi}_{C}\right)$$

$$\tilde{\phi}_{f} = 1 \qquad \qquad \frac{\tilde{\xi}_{C}}{\tilde{\xi}_{f}} \left(1 + \tilde{\xi}_{f} - \tilde{\xi}_{C}\right) < \tilde{\phi}_{C} < 1$$

$$\tilde{\phi}_{f} = \tilde{\phi}_{C} \qquad \text{elsewhere}$$

SKEW VERY HIGH RESOLUTION SCHEMES

Details regarding the family of skew VHR schemes can be found in Ref. [11]. A brief description of the construction of these schemes is given next.

Streamline-Based Interpolation

As mentioned above, the VHR family of schemes is an extension of the one-dimensional HR family into multidimensional spaces. Therefore, in order to be able to apply the various HR schemes in streamline-based coordinates, ϕ estimates at three locations (two upstream and one downstream) in the direction of the local velocity vector are needed. For that purpose, the direction of the velocity vector at the cell face is considered to determine the streamline direction, and interpolation is carried among the appropriate nodes surrounding the cell face to obtain the upstream (ϕ_U) , central (ϕ_C) , and downstream (ϕ_D) nodal values in the skew direction (Figure 1a).

Using these interpolated estimates, the value at the control volume face is calculated employing expressions similar to those of the HR schemes. However, the local coordinate system used is no longer the mesh coordinate system but rather the streamline coordinate system. For more details, the reader is referred to Ref. [11].

Having obtained the necessary values in the streamline direction, the following normalized variables [11] are used in place of those defined in Eq. (10), in order to apply the functional relationships of HR schemes along that direction in a bounded manner:

$$\underline{\tilde{\phi}} = \frac{\phi - \underline{\phi}_{\mathsf{U}}}{\underline{\phi}_{\mathsf{D}} - \underline{\phi}_{\mathsf{U}}} \qquad \underline{\tilde{\xi}} = \frac{\xi - \underline{\xi}_{\mathsf{U}}}{\underline{\xi}_{\mathsf{D}} - \underline{\xi}_{\mathsf{U}}} \tag{24}$$

Bounding Strategy

When calculating ϕ_f using the original HR schemes, the upstream, central, and downstream nodal values are available and need not be interpolated. In streamline-based coordinates, however, estimates at these locations, as mentioned earlier, are not available and should be obtained by interpolation. Since a linear interpolation profile is used, the resulting control volume face value may not always be bounded in the physical sense (i.e., even though the CBC is enforced along the streamline direction, the calculated face value can still be outside the range set by the two points neighboring the face). In order to eliminate any unphysical results, after the calculation of $\tilde{\phi}_f$ using any of the above schemes, the face value is denormalized to yield ϕ_f , and then the CBC is enforced using the appropriate nodal values (ϕ_U , ϕ_C , and ϕ_D (Figure 1a)) in the event it is not satisfied.

NORMALIZED ADAPTIVE CRITERION

An important ingredient of any adaptive technique is the switching criterion. As mentioned earlier, skew schemes greatly improve predictions in regions where the flow is skew with respect to the grid lines. Therefore the skewness of the flow with respect to the grid should be reflected in the switching criterion. Moreover, the skewness alone is not a sufficient parameter for adaptation because skew flow regions of slow changes in the gradient values are well predicted even with first-order schemes. Consequently, spatial variations in the dependent variable should also be accounted for if the switching criterion is to be an effective one.

The skewness of the grid with respect to the flow direction is accounted for in the switching criterion through a parameter denoted by SLOPE. This represents the angle between the velocity vector and the line segment joining the central and downstream grid points surrounding the control volume face. Moreover, regions in the flow field characterized by higher changes in the gradient values as compared to other regions, could be captured via the following parameter that measures the absolute value of the gradient across the cell face of the finite volume:

$$GRAD_{f} = \left| \frac{\phi_{D} - \phi_{C}}{\xi_{D} - \xi_{C}} \right|$$
 (25)

The problems with using GRAD were thoroughly investigated by Darwish and Moukalled [22] and are briefly reviewed here. First, for similar profiles with different maximum values, different values of GRAD (that are directly proportional to the levels of the profiles) are obtained. Therefore the GRAD parameter cannot be used in an absolute manner to decide on where to adapt. Thus, to obtain the same GRAD values for two similar profiles, the ϕ field should be scaled or normalized. Another difficulty arises when calculating the GRAD parameter for the same profile using different grid networks. In this case, the difference in the grid spacing affects the value of GRAD, with the coarser grid showing lower GRAD levels and thus not making use of the more accurate scheme as much as the denser grid, which is contrary to the actual requirements. Hence the local coordinate should be normalized as well.

To overcome the above mentioned shortcomings, the normalization procedure developed by Darwish and Moukalled [22] is adopted in this work, whereby the gradient over the interface is compared to the gradient obtained from the two next points as if the gradient of the interface was calculated using a coarser grid. In this case the normalized gradient parameter becomes

$$\overline{GRAD}_{f} = \frac{\left| \frac{\phi_{D} - \phi_{C}}{\xi_{D} - \xi_{C}} \right|}{\left| \frac{\phi_{DD} - \phi_{U}}{\xi_{DD} - \xi_{U}} \right|}$$
(26)

Results generated using the normalized gradient parameter [22] revealed that estimates of GRAD are the same in all cases, indicating the possibility of setting a

universal value for \overline{GRAD} beyond which adaptation can be performed. The only difficulty that arises is when the maximum value of the profile is very small, in which case adaptation will be unnecessarily required. To overcome this problem, the GRAD value is used as a filtering parameter, i.e., if the numerator is less than a threshold value, the normalized gradient (\overline{GRAD}) is set to zero, thus avoiding any artificially high value.

STRATEGY FOR ADAPTIVE SCHEMES

The adaptive strategy developed in this work consists of using the HR scheme in solving the equations until the residual error drops to a set level; then the solution field is employed to calculate the SLOPE and \overline{GRAD} switching parameters for one time and to delimit control volume faces where the VHR scheme should be applied. For the computations presented in this article, control volume faces are flagged if the SLOPE is between 30° and 60° and the \overline{GRAD} is greater than 0.7. Moreover, the \overline{GRAD} is calculated for every dependent variable in the problem. Therefore different variables have different flagged areas.

The use of the SLOPE alone is not a sufficient indicator for adaptation, since regions where the flow may be skewed to the grid lines and the gradient of the dependent variable are not important do not represent critical regions of the flow field. The pure convection of a step profile in an oblique flow field problem is an excellent example of such a case in which the important region of the flow field is along the step. As shown below, the current switching criterion accurately predicts this region. Using the slope alone would have resulted in flagging the whole domain.

As mentioned above, the criterion is applied once to delimit regions where the VHR scheme should be employed. The reason behind this strategy is to avoid convergence problems that arise from oscillation between the HR and the VHR scheme. The other reason is that using the criterion before the residual of the field has been lowered enough is not useful, since it would be based on values that are far from the converged solution field. Moreover, experimentation showed that applying the adaptive criterion more frequently unnecessarily increases the computation cost without improving the accuracy.

It should be clarified here that all adaptive schemes tested in this article are composed of the same scheme applied in its one-dimensional and multidimensional forms. However, the methodology is not limited to that, and actually, any HR scheme can be used with any VHR scheme adaptively.

IMPLEMENTATION OF THE ADAPTIVE SCHEMES

When constructing cost-effective highly accurate adaptive schemes, it is important to pay attention to their implementation so as to make sure they can be easily coded in current programs and that the solution of the discretized equations can be readily accomplished with a high rate of convergence.

In this work, for convection-diffusion type problems, two techniques are used in tandem to implement the AVHR schemes. These methods are the deferred-

correction (DC) procedure of Rubin and Khosla [18] and the normalized weighting factor (NWF) technique developed by the authors [17]. The NWF is an acceleration technique that was shown [17] to speed up the convergence rate by a factor of 4. This method, however, still needs some work to be extended to flow problems and is currently under consideration by the authors. Consequently, when solving flow problems, the DC method is used alone to implement the AVHR schemes. Both implementation techniques were described in previous articles [17, 22] and will not be repeated here.

RESULTS AND DISCUSSION

To check the performance of the new AVHR schemes against their VHR counterparts, one purely convective problem and three flow problems are solved. Results are obtained by covering the physical domains with uniform grids. Grid networks are generated using the transfinite interpolation technique [25]. In all tests, computational results are considered converged when the residual error (RE), defined as

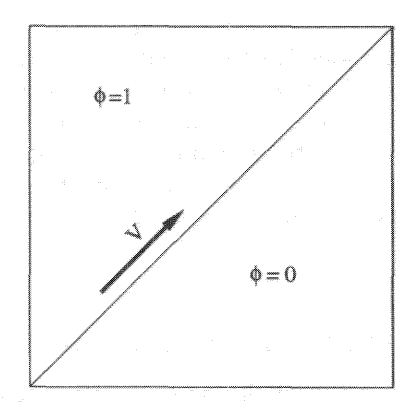
$$RE = \max_{i=1}^{n} \left[\left| a_{D} \phi_{D} - \left(\sum_{NB} a_{NB} \phi_{NB} + b_{D} + q b_{dc} \right) \right| \right]$$
 (27)

where q = 1 for the DC approach and q = 0 for the NWF method, became smaller than a vanishing quantity (10^{-5}) .

Before presenting and discussing results, it should be made clear that the objective of the article is to develop and test a new family of AVHR schemes. Since the new family is streamline based, it is natural to choose the flow in some of the test problems to be skewed to the grid lines. Furthermore, the skew VHR schemes were shown in Ref. [11] to be more accurate than the one-dimensional HR schemes. Therefore, in order not to overload plots, comparison will be limited here to results generated by the VHR and AVHR schemes.

Test 1: Pure Convection of a Step Profile in an Oblique Velocity Field

Figure 2a shows the well-known benchmark test problem consisting of pure convection of a transverse step profile for a scalar quantity ϕ imposed at the inflow boundary of a square computational domain. A 21×21 mesh system is used, the angle θ is chosen to be 45° , and |V|=1. The problem is solved using the following four schemes: MINMOD, CLAM, SMART, and SHARP. Comparisons of the computation time obtained for the VHR and AVHR solutions of the problem using these schemes are displayed graphically in Figure 2b. As shown, important economies are achieved with the adaptive schemes as compared to the skew schemes. The reduction in cost varies from 33.7% for the SMART scheme to 55.46% for the CLAM scheme, with an average savings of 48.17%. The validity of the adopted switching criterion is clearly demonstrated by the flagged areas



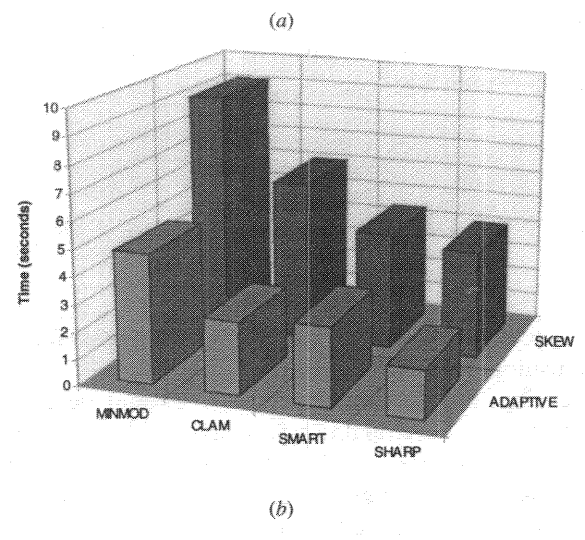


Figure 2. (a) Physical domain for pure convection of a scalar discontinuity. (b) Time comparison for pure convection of a scalar discontinuity.

displayed in Figure 3. As shown, only regions across the step are flagged, with the largest flagged area being associated with the most diffusive scheme (i.e., the MINMOD scheme). Finally, the computed values of ϕ using the VHR schemes, the AVHR schemes, and the exact solution to the problem are shown, along the vertical centerline of the domain, in Figure 4. Results displayed in the figure show that estimates generated by the AVHR schemes fall right on top of those generated by the more expensive VHR schemes. Therefore the savings in computation cost with the AVHR schemes are achieved without deteriorating the solution accuracy.

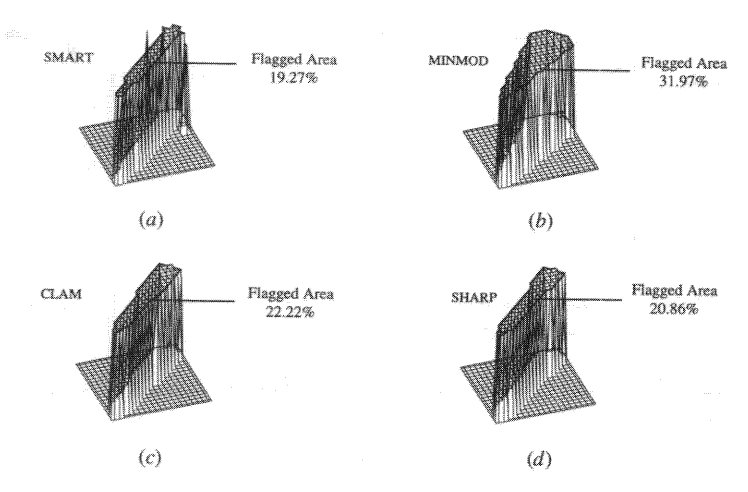


Figure 3. Flagged areas for pure convection of a scalar discontinuity problem.

Test 2: Laminar Driven Flow in a Skew Cavity

A schematic of the physical situation and streamlines are depicted in Figure 5a. Results are presented for a value of Reynolds number (Re = $\rho UL/\mu$, L being the cavity height or width and U the velocity of the top horizontal wall) of 500. The side walls are skewed at an angle of 50° with respect to the horizontal. The problem is solved using the SUPERC, STOIC, OSHER, and SMART schemes and two grid networks of sizes 22×22 and 42×42 . Comparisons of the computation time obtained for the VHR and AVHR solutions of the problem using these schemes are displayed graphically in Figure 5b. For the 22×22 grid the reduction in cost with the AVHR schemes as compared to the VHR schemes varies from 50.31% for the SUPERC scheme to 62.11% for the OSHER scheme, with an average savings of 57.13%. For the 42×42 grid, the minimum and maximum reduction in cost are 50.78% (SMART) and 60.92% (SUPERC), respectively, with the average being 57.94%. Therefore important savings in the computation time needed to solve this flow problem are achieved with the adaptive schemes. To check whether these savings affect the solution accuracy, the U velocity profiles along the vertical centerline of the domain generated by the VHR and AVHR schemes using both grid layouts are compared, in Figure 6, against the profile predicted by SMART using a very dense grid of size 242×242 . For all schemes and on both grids, the AVHR and VHR solutions fall on top of each other, indicating that this decrease in computation cost is attained without affecting the accuracy of the solution.

Test 3: Laminar Sudden Expansion of an Oblique Flow Field in a Rectangular Cavity

The physical situation under consideration along with the flow field are displayed in Figure 7a. The flow is assumed to be steady, laminar, and two-dimen-

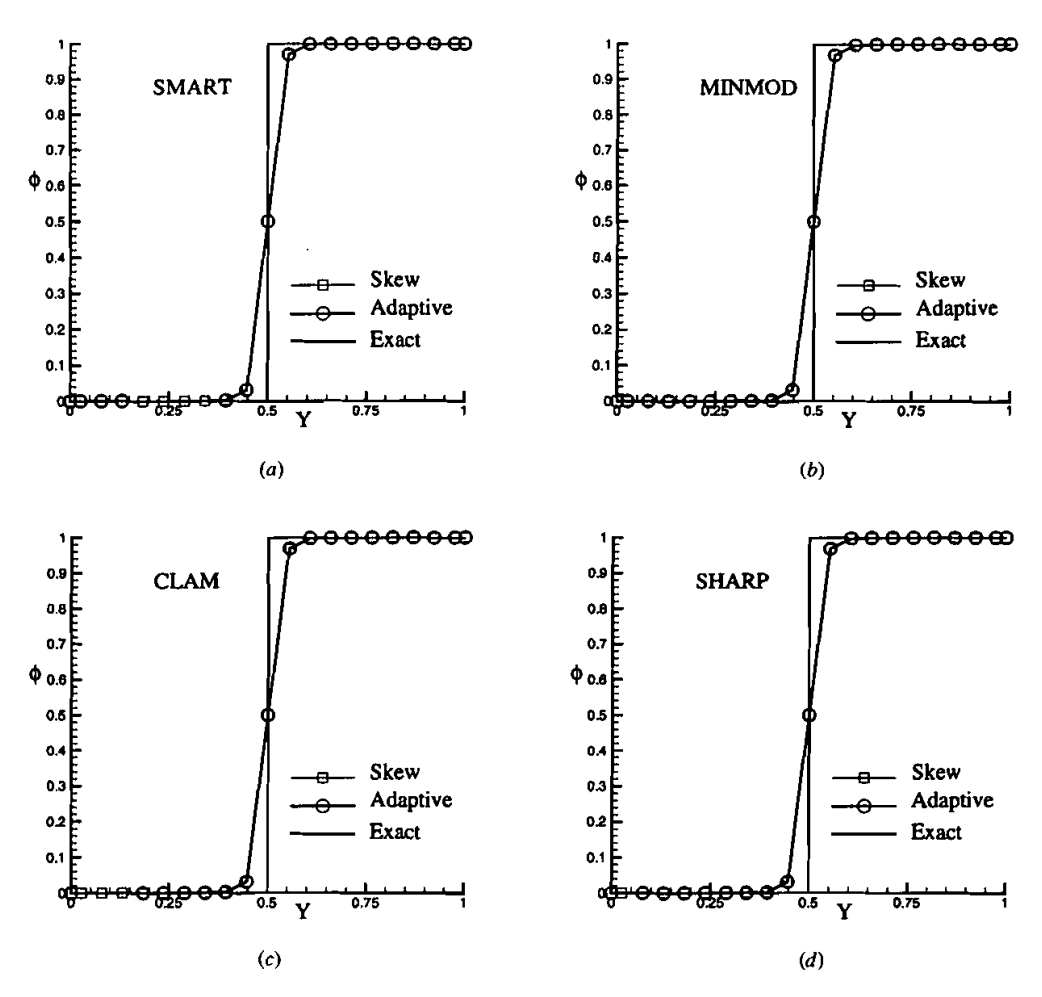


Figure 4. Values of ϕ along the vertical centerline of the domain for the pure convection of a scalar discontinuity problem.

sional. The problem is solved using the MUSCL and MINMOD schemes in their AVHR and VHR forms for a value of Reynolds number (Re = $\rho VL/\mu$, L being the cavity height or width and V the reference velocity) of 500. As in the previous test problem, two uniform grid systems of sizes 22 × 22 and 42 × 42 are used.

The time required to solve the problem by both schemes is depicted in Figure 7b. For the 22×22 grid the use of the adaptive approach reduces the cost by 47.63% for the MUSCL scheme and by 57.90% for the MINMOD scheme, with an average savings in computation power of 53.05%. These values are 40.11% and 32.25%, respectively, for the 42×42 grid, with an average savings of 36.5%. The accuracy of the solution of the adaptive scheme is checked through the U velocity

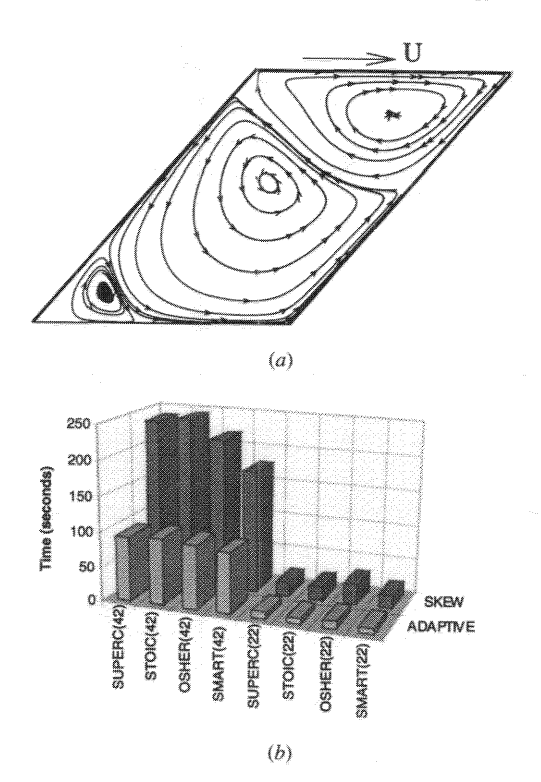


Figure 5. (a) Physical domain and streamlines for the driven flow in a skew cavity problem (Re = 500). (b) Time comparison for the driven flow in a skew cavity problem.

profiles along the vertical centerline of the domain presented in Figure 8 for both grid layouts. These values are also compared against the solution generated by the SMART scheme using a very dense grid of size 242 × 242. For both schemes and on both grids, the AVHR and VHR solutions coincide, verifying that this reduction in computation cost is accomplished without touching the accuracy of the solution.

Test 4: Turbulent Sudden Expansion of an Oblique Flow Field in a Rectangular Cavity

The physical domain for this problem, illustrated schematically in Figure 9a, is the same as that in Test 3; however, the working fluid is assumed to enter the domain with a high velocity, resulting in a fully turbulent flow field. Without going into details, the two-equation k- ε turbulence model [24] is invoked in the flow solver to evaluate the turbulent viscosity and Reynolds stresses, and the law of the wall is used at the walls. The time-averaged equations governing the flow field are solved using the SMART and EXPONENTIAL schemes in their AVHR and VHR

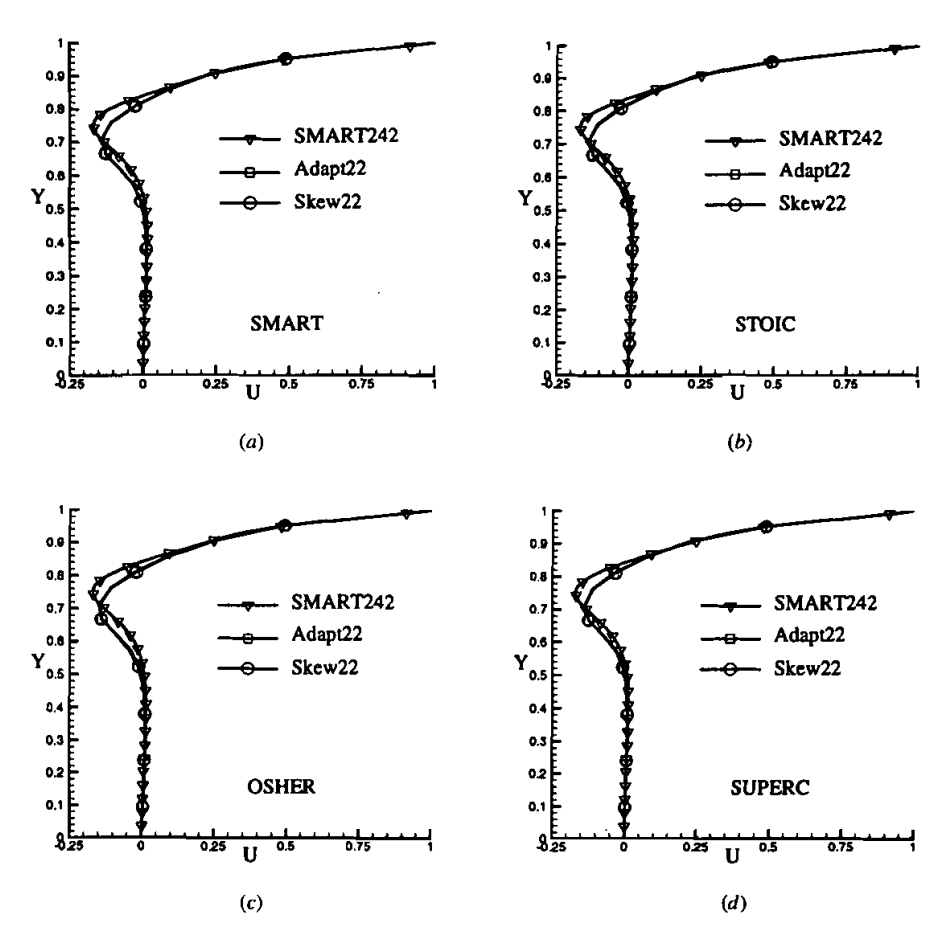


Figure 6. Comparison of the U velocity profiles along the vertical centerline of the domain for the driven flow in a skew cavity problem.

forms for a value of Reynolds number (Re = $\rho VL/\mu$, L being the cavity height or width and V the reference velocity) of 50,000. Three uniform grid systems of sizes 22×22 , 42×42 , and 62×62 are used.

The computation time needed to solve the problem by both schemes is depicted in Figure 9b. Important reduction in cost is realized on all grids with the AVHR schemes. For the SMART scheme, savings vary with the increase in grid size from 33.6% up to 66.78% and then down to 52.03%. For the EXPONENTIAL scheme these values are 19.86%, 46.59%, and 37.27%, respectively. The average savings vary with the increase in grid size from 27.32% up to 56.79% and then down to 44.73%. Therefore, for all grid sizes tested in this work, the adaptive schemes appreciably reduce the computation time required to solve the turbulent flow problem. The accuracy of the solution of the adaptive schemes is checked by

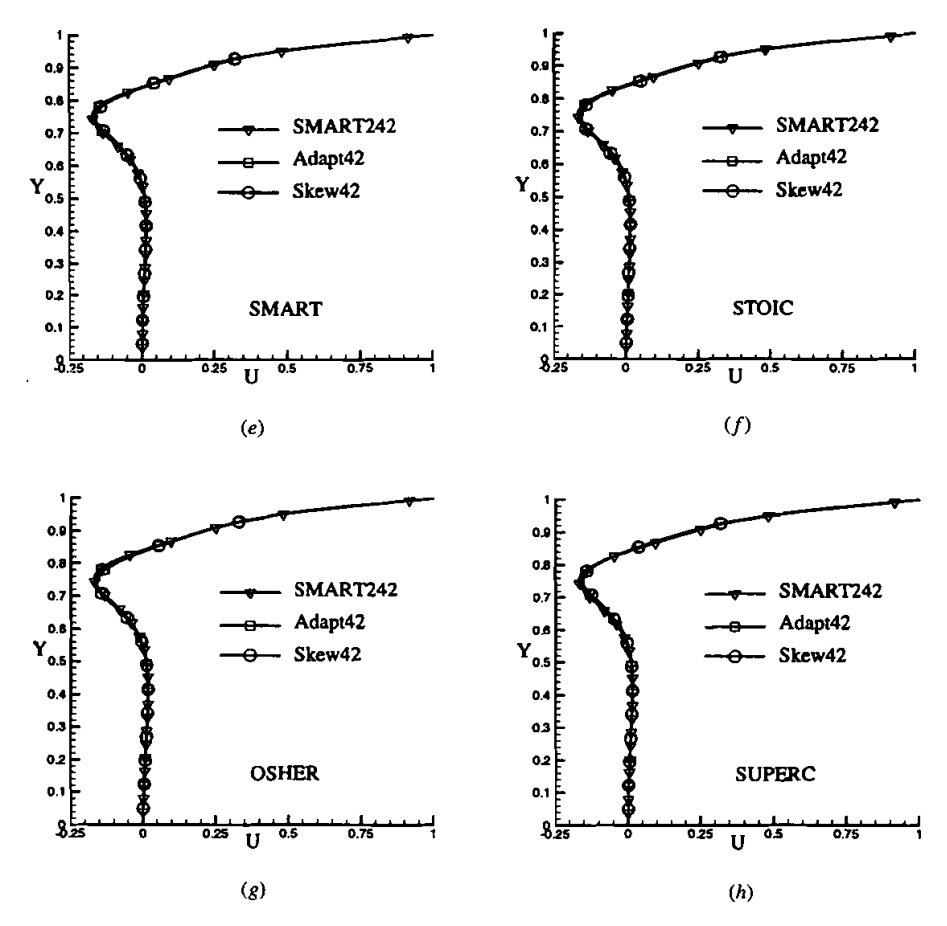
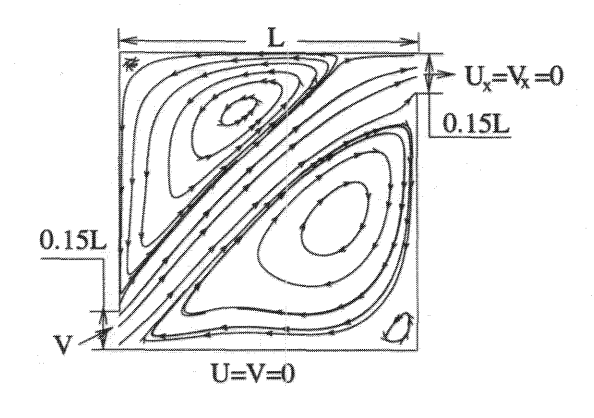


Figure 6. Comparison of the U velocity profiles along the vertical centerline of the domain for the driven flow in a skew cavity problem (Continued).

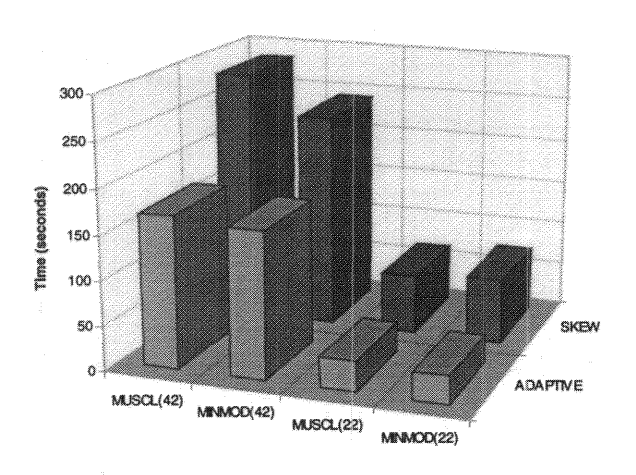
presenting, for all grid sizes, the U velocity profiles along the vertical centerline of the domain (Figure 10) in addition to the solution generated by the SMART scheme using a very dense grid of size 242×242 . In all cases, the AVHR and VHR solutions fall on top of each other, verifying once more that this reduction in computation cost is accomplished without deteriorating the accuracy of the solution. Finally, the overall reduction in cost, defined as the difference between the total time needed to solve all problems presented using the VHR schemes and the AVHR schemes divided by the time needed by the VHR schemes, is found to be 48.74%.

CLOSING REMARKS

A new family of adaptive very high resolution schemes was developed. This was done by adaptively combining the family of high resolution schemes with the family of skew very high resolution (VHR) schemes via a new adaptive switching



(a)



(b)

Figure 7. (a) Physical domain and streamlines for laminar sudden expansion in a rectangular cavity (Re = 500). (b) Time comparison for laminar sudden expansion in a rectangular cavity.

criterion. The performance of the new family was compared in terms of accuracy and computation cost against that of the VHR base family of schemes by solving four problems. For the same accuracy, important economies were achieved with the new family for all cases tested. The overall savings in computation time was found to be 48.74%.

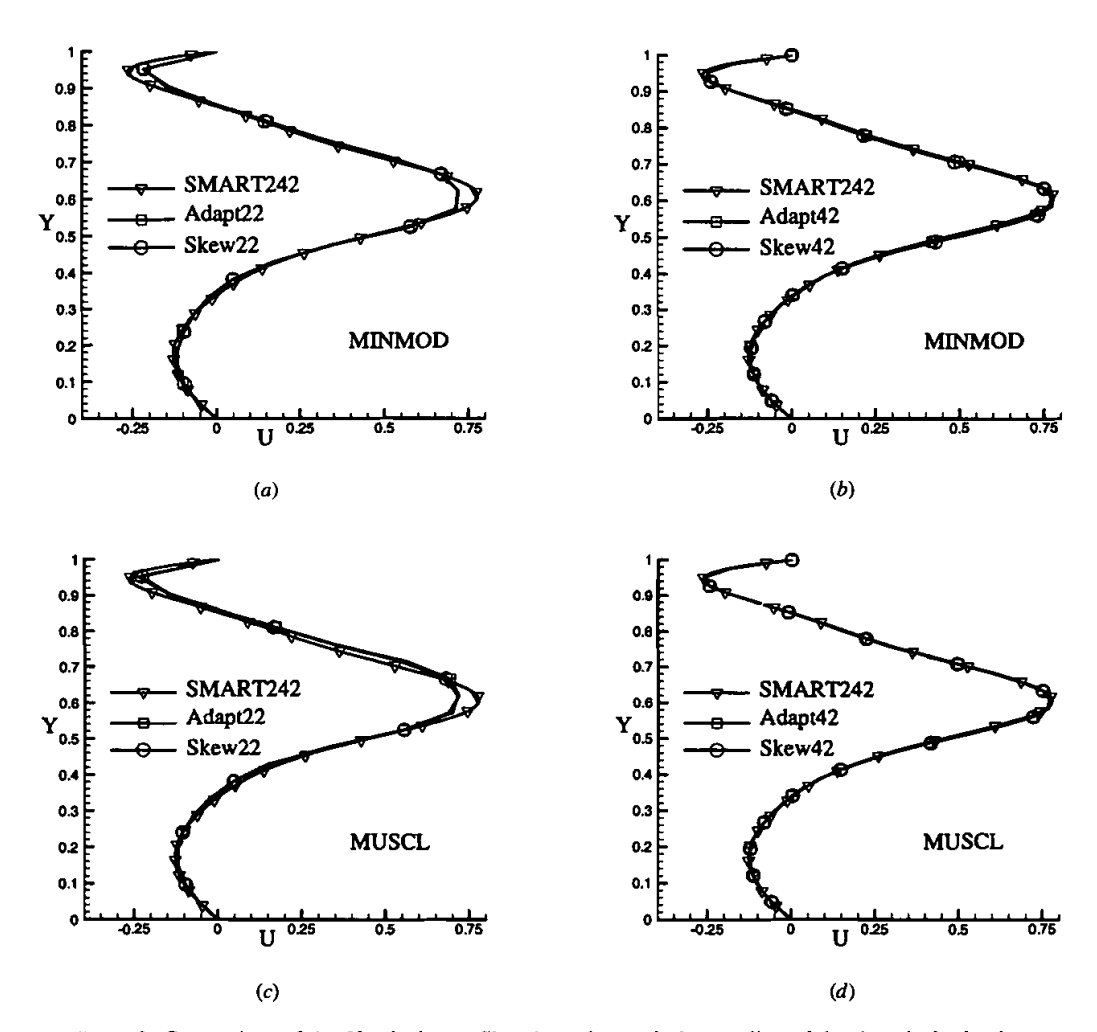


Figure 8. Comparison of the U velocity profiles along the vertical centerline of the domain for laminar sudden expansion in a rectangular cavity (Re = 500).

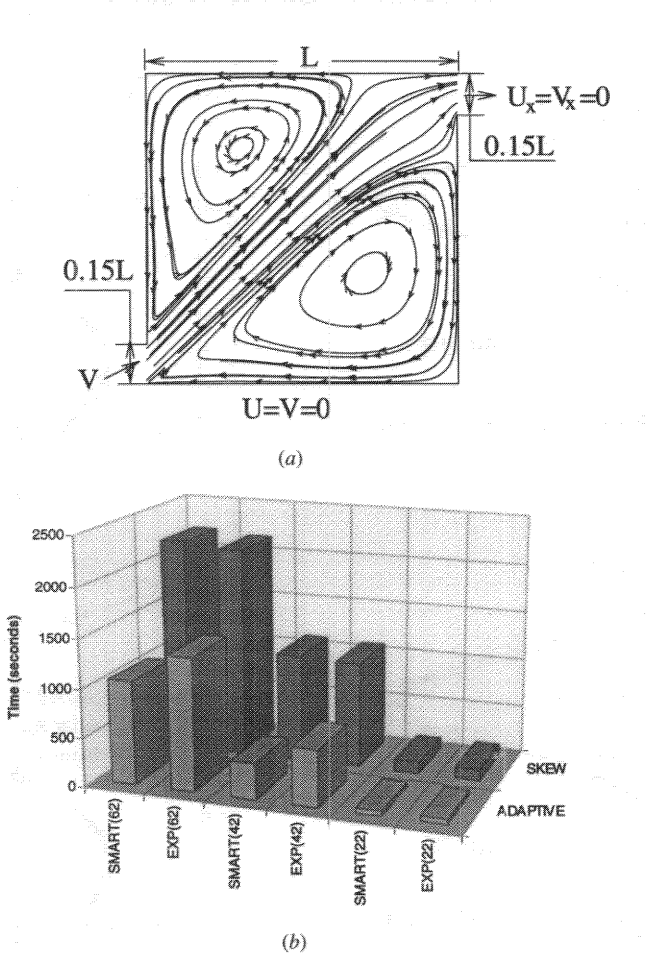


Figure 9. (a) Physical domain and streamlines for turbulent sudden expansion in a rectangular cavity (Re = 50,000). (b) Time comparison for turbulent sudden expansion in a rectangular cavity.

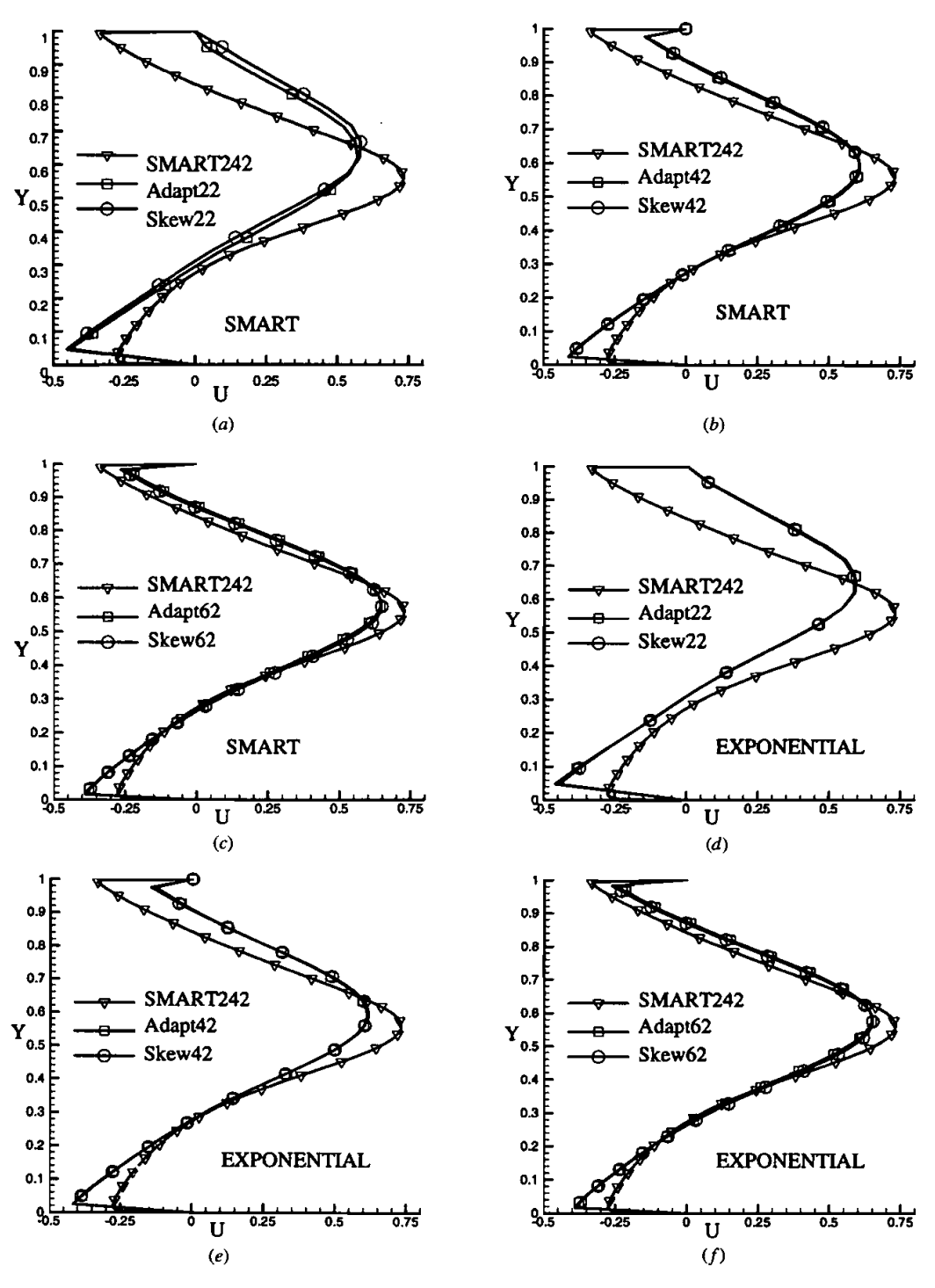


Figure 10. Comparison of the U velocity profiles along the vertical centerline of the domain for turbulent sudden expansion in a rectangular cavity (Re = 50,000).

REFERENCES

- 1. B. Van Leer, Towards the Ultimate Conservative Difference Scheme: II—Monotonicity and Conservation Combined in a Second Order Scheme, *J. Comput. Phys.*, vol. 14, pp. 361-370, 1974.
- 2. B. Van Leer, Towards the Ultimate Conservative Difference Scheme: V—A Second-Order Sequel to Godunov's Method, J. Comput Phys., vol. 23, pp. 101-136, 1977.
- 3. S. R. Chakravarthy and S. Osher, High Resolution Applications of the OSHER Upwind Scheme for the Euler Equations, AIAA Paper 83-1943, 1983.
- 4. A. Harten, High Resolution Schemes for Hyperbolic Conservation Laws, *J. Comput. Phys.*, vol. 49, pp. 357–393, 1983.
- 5. B. P. Leonard and S. Mokhtari, Beyond First-Order Upwinding: The Ultra-Sharp Alternative for Non-Oscillatory Steady-State Simulation of Convection, *Int. J. Numer. Methods Eng.*, vol. 30, pp. 729-766, 1990.
- 6. P. H. Gaskell and A. K. C. Lau, Curvature Compensated Convective Transport: SMART, a New Boundedness Preserving Transport Algorithm, *Int. J. Numer. Methods Fluids*, vol. 8, pp. 617-641, 1988.
- 7. M. S. Darwish, A New High Resolution Scheme Based on the Normalized Variable Formulation, *Numer. Heat Transfer Part B*, vol. 24, pp. 353-371, 1993.
- 8. B. P. Leonard, Locally Modified Quick Scheme for Highly Convective 2-D and 3-D Flows, in C. Taylor and K. Morgan (eds.), *Numerical Methods in Laminar and Turbulent Flows*, vol. 5, pp. 35-47, Pineridge Press, Swansea, England, 1987.
- B. P. Leonard, The ULTIMATE Conservative Difference Scheme Applied to Unsteady One-Dimensional Advection, Comput. Methods Appl. Mech. Eng., vol. 88, pp. 17-74, 1991.
- F. Moukalled and M. Darwish, New Bounded Skew Central Difference Scheme, Part I: Formulation and Testing, Numer. Heat Transfer, Part B, vol. 31, no. 1, pp. 91-110, 1997.
- 11. F. Moukalled and M. Darwish, A New Family of Streamline-Based Very-High Resolution Schemes, *Numer. Heat Transfer, Part B*, vol. 32, pp. 299-320, 1997.
- 12. P. K. Sweeby, High Resolution Schemes Using the Flux Limiters for Hyperbolic Conservation Laws, SIAM J. Numer. Anal., vol. 21, pp. 995-1011, 1984.
- 13. M. S. Darwish and F. Moukalled, Normalized Variable and Space Formulation Methodology for High-Resolution Schemes, *Numer. Heat Transfer*, *Part B*, vol. 26, pp. 79-96, 1994.
- Y. N. Jeng and U. J. Payne, An Adaptive TVD Limiter, J. Comput. Phys., vol. 118, pp. 229-241, 1995.
- 15. T. Rhodes and S. Acharya, An Adaptive Differencing Scheme for Flow and Heat Transfer Problems, *Numer. Heat Transfer, Part B*, vol. 23, pp. 153-173, 1993.
- S. Mokhtari, Development and Analysis of Steady High-Resolution Non-Oscillatory Convection Schemes Using Higher-Order Upwinding, Ph.D. dissertation, University of Akron, 1991.
- 17. M. S. Darwish and F. Moukalled, The Normalized Weighting Factor Method: A Novel Technique for Accelerating the Convergence of High-Resolution Convective Schemes, *Numer. Heat Transfer, Part B*, vol. 30, pp. 217–237, 1996.
- 18. S. G. Rubin and P. K. Khosla, Polynomial Interpolation Method for Viscous Flow Calculations, *J. Comput. Phys.*, vol. 27, pp. 153-168, 1982.
- M. Peric, A Finite Volume Method for the Prediction of Three-Dimensional Fluid Flow in Complex Ducts, Ph.D. thesis, Mechanical Engineering Department, Imperial College, 1985.
- 20. J. P. Van Doormal and G. D. Raithby, Enhancements of the SIMPLE Method for Predicting Incompressible Fluid Flow, *Numer. Heat Transfer*, vol. 7, pp. 147-163, 1984.

- 21. S. V. Patankar, Numerical Heat Transfer and Fluid Flow, Hemisphere, Washington, D.C., 1981.
- 22. M. S. Darwish and F. Moukalled, An Efficient Very-High-Resolution Scheme Based on an Adaptive-Scheme Strategy, *Numerical Heat Transfer*, *Part B: Fundamentals*, vol. 34, pp. 191–213, 1998.
- 23. W. J. Gordon and L. C. Thiel, Transfinite Mappings and Their Applications to Grid Generation, in Thompson, J. F. (ed.), *Numerical Grid Generation*, pp. 171-192, North Holland, New York, 1982.
- 24. B. E. Launder and D. B. Spalding, The Numerical Calculation of Turbulent Flows, Comput. Methods Appl. Mech. Eng., vol. 3, pp. 269-289, 1974.